Thermal resistance of fiber-reinforced reactive powder concrete with marble powder waste

by Widodo Kushartomo

Submission date: 18-Nov-2026 11:11AM (UTC+0700)
Submission ID: 3093038335
File name: Artikel.pdf (3.62M)
Word count: 6741
Character count: 40465

Advances in Concrete Construction, *Vol. 22, No. 5 (2026) 533-548*
https://doi.org/10.12989/acc.2026.22.5.01

Techno-Press

Thermal resistance of fiber-reinforced reactive powder concrete with marble powder waste

Widodo Kushartomo*[1], Andy Prabowo[1], Yohannes L. Yaphary[2,3]

[1]*Department of Civil Engineering, Universitas Tarumanagara, No. 1 Let. Jend. S. Parman, West Jakarta, 1440, Indonesia*
[2]*Department of Chemistry, National University of Singapore, 3 Science Drive 3, 117543, Singapore*
[3]*Element Construction Testing (S) Pte. Ltd., 4 Tuas Loop, Tuas Connection, 637342, Singapore*

(Received September 25, 2025, Revised September 21, 2026, Accepted September 29, 2026)

Abstract. Marble powder is an increasingly significant industrial waste and has shown potential for beneficial incorporation into reactive powder concrete (RPC). However, the elevated-temperature behavior of RPC incorporating marble powder remains relatively understudied. In particular, the performance of marble-powder RPC reinforced with commonly used steel and polypropylene (PP) fibers under elevated-temperature exposure remains insufficiently understood. This study therefore investigates the distinct effects of steel and PP fibers at different dosages on the spalling resistance and residual compressive strength of fiber-reinforced RPC (FRPC) incorporating marble powder after exposure to elevated temperatures. Steel fibers improved the compressive strength of RPC up to 300°C but suffered rapid deterioration beyond this threshold, compromising material integrity. In contrast, PP-reinforced RPC (PFRPC) exhibited superior thermal stability, effectively mitigating spalling up to 400°C despite having minimal impact on ambient compressive strength. Optimal fiber contents were identified as 1.00% steel and 0.10% PP for maximum spalling resistance, while 1.50% steel and 0.15% PP maximized compressive strength retention. In relation to temperature exposure of class ratings (T-ratings), the effective performance of SFRPC up to 300°C corresponds to the maximum surface-temperature limit associated with the T2 class, whereas PFRPC maintained its integrity at 400°C, approaching the 450°C maximum surface-temperature limit associated with the T1 class. These findings provide useful material-level insights for selecting steel and PP fibers and optimizing thermally resistant FRPC for structural or protective construction, considering thermal resistance and mechanical resilience in thermally demanding environments.

Keywords: elevated temperature; marble powder; polypropylene; reactive powder concrete; steel

1. Introduction

The rapid growth of urban populations and the increasing prevalence of densely occupied multifunctional buildings have significantly driven up energy demand. Consequently, adopting low-energy practices has become a key priority in transforming the construction industry to mitigate energy shortages [1, 2]. Modern buildings utilize advanced thermal insulation to regulate heat transfer between zones, optimizing energy consumption for heating, ventilation, and air conditioning (HVAC) and mitigating fire hazards associated with temperature-sensitive materials.

*Corresponding author, Ph.D., E-mail: widodo@untar.ac.id

Copyright © 2026 Techno-Press
http://www.techno-press.org/acc/5

ISSN: 2287-5301 (Print), 2287-531X (Online)

In hazardous areas where flammable gases or vapors may be present, control of equipment surface temperature is particularly important because excessively high surface temperatures may provide a potential ignition source. Temperature class ratings (T-ratings) therefore specify the maximum permissible surface temperature of equipment intended for use in such environments [3]. Under the ATEX Directive, these classifications play a crucial role in explosion protection by limiting allowable temperatures in hazardous zones. The ATEX framework consists of two directives: ATEX 114 (Directive 2014/34/EU), which governs equipment and protective systems intended for use in explosive atmospheres, and ATEX 153 (Directive 1999/92/EC), which establishes workplace safety requirements for workers in explosive environments. The T-ratings range from T1, corresponding to a maximum equipment surface temperature of 450°C, to T6, corresponding to 85°C. Thermal insulation and protective construction are important for controlling heat transfer and maintaining surface temperatures within the applicable T-class limits. However, under abnormal or severe thermal conditions, such as fire or excessive heat exposure, these temperature limits may be exceeded. Where concrete forms part of the surrounding structural or protective construction, deterioration, cracking, or spalling may impair its ability to maintain physical separation and provide continued protection to adjacent equipment and areas. Therefore, the resistance of concrete to thermal deterioration and loss of mechanical integrity becomes an important consideration in thermally demanding and hazardous environments.

Cementitious materials are inherently more resilient as thermal insulating materials than many other construction materials, but their performance under thermal stress depends on proper material design [4]. In recent decades, the demand for reactive powder concrete (RPC) has surged in the construction industry due to its superior performance [5, 6]. RPC, a high-strength cementitious composite developed in the 1990s, is characterized by ultra-high strength, remarkable deformability, and outstanding durability [7]. However, the high cement content of RPC contributes to its environmental footprint and economic challenges [8]. Partial Portland cement replacement with industrial byproducts has been explored to enhance sustainability and cost-effectiveness [9]. Among these alternatives, marble powder, a byproduct of cutting and polishing processes in marble factories, presents a promising recycling opportunity [10]. Its increasing production raises environmental concerns, necessitating valorization strategies for reuse in construction materials to reduce waste and mitigate pollution [11].

Marble powder waste is a calcium-carbonate-rich ($CaCO_3$) material and, unlike ordinary Portland cement (OPC), does not provide the same primary cementitious contribution during hydration. Nevertheless, previous studies have reported that, at an appropriate replacement level, marble powder can partially replace OPC while maintaining, and in some cases improving, the performance of cement-based materials [12]. This demonstrates its potential as a beneficial supplementary material for reducing OPC consumption while maintaining the required material performance. Although the beneficial effect depends on the replacement level, with excessive substitution potentially affecting mechanical performance [13], the partial replacement of OPC with marble powder provides an important environmental advantage by reducing OPC consumption and its associated environmental burden while simultaneously providing a beneficial reuse pathway for marble-processing waste. The utilization of marble powder waste can therefore contribute to reducing conventional raw-material consumption, promoting waste recycling, and supporting circular-economy practices [14]. These benefits are particularly relevant to RPC because its characteristically high cement content contributes substantially to its environmental footprint.

Despite its exceptional mechanical performance, RPC is highly susceptible to thermal spalling

when exposed to temperatures exceeding 300°C, which may result in severe material deterioration and explosive spalling [15, 16]. In RPC applications, spalling-induced material loss poses an even greater risk as the structural elements are designed with reduced cross-sectional areas due to RPC's inherently high strength [17]. To mitigate spalling and enhance elevated-temperature performance, fibers are widely incorporated into fiber-reinforced RPC (FRPC), reinforcing its structural integrity under extreme thermal conditions [18, 19]. Steel and polypropylene (PP) fibers dominate FRPC applications among various fiber types due to their well-documented effectiveness in improving thermal stability [19-21].

While the elevated-temperature behavior of conventional FRPC has been extensively investigated, considerably less attention has been given to FRPC incorporating marble powder waste. In particular, the performance of marble-powder RPC reinforced with steel and PP fibers under elevated-temperature exposure remains insufficiently understood. This knowledge gap is important because steel and PP fibers provide fundamentally different reinforcing mechanisms, and their effectiveness may vary as thermal deterioration of the marble-powder RPC matrix progresses.

This study addresses this knowledge gap by systematically investigating the individual effects of steel and PP fibers at different dosages on the elevated-temperature performance of RPC incorporating marble powder waste. Steel-fiber-reinforced RPC (SFRPC) and PP-fiber-reinforced RPC (PFRPC) were separately evaluated and compared in terms of spalling resistance and residual compressive strength after exposure to elevated temperatures. By distinguishing the temperature-dependent performance of the two fiber systems and evaluating the influence of fiber dosage, this study provides a comparative basis for selecting fiber type and content for marble-powder RPC subjected to elevated-temperature conditions. The findings contribute to the development of more thermally resistant FRPC while supporting the beneficial utilization of marble powder waste in high-performance cementitious materials.

2. Materials and methods

2.1 Materials

The Type I Portland cement used in this study complied with ASTM C150 (2022) and was sourced from PT Indocement Tunggal Prakarsa Tbk., Jakarta, Indonesia. The silica fume used in this study complied with ASTM C1240 (2020) and was supplied under the commercial name SikaFume by PT. Sika Indonesia, West Java, Indonesia. Marble powder, a byproduct of marble cutting and polishing processes, was obtained from a local marble processing facility in Purwakarta, West Java, Indonesia. A polycarboxylate-based superplasticizer, MasterGlenium SKY 8851 supplied by PT BASF Indonesia, Jakarta, Indonesia, was used to enhance workable consistency. The fine aggregate, a quartz river sand, was sourced from Bangka, Bangka Belitung Islands, Indonesia. To ensure uniform particle size distribution, the sand was sieved to pass through Sieve No. 40, in accordance with ASTM E11 (2022). The physical properties of the marble powder and sand are presented in Table 1. The marble powder properties were obtained from the supplier, while the specific gravity and water absorption of the sand were determined following ASTM C128 (2022).

The steel fibers used in this study were supplied by Ganzhou Daye Metallic Fibres Co., Ltd., Jiangxi, China, measuring 13 mm in length and 0.12 mm in diameter, with a tensile strength

Table 1. Physical properties of sand and marble powder

Material	Specific gravity	Maximum particle size (mm)	Absorption (%)
Marble powder	3.060	0.015	-
Sand	2.600	0.425	1.7



Figure 1. Physical appearances of steel and polypropylene (PP) fibers

Table 2. Normalized mix design of reactive powder concrete (RPC) based on cement weight, with a water-to-binder ratio of 0.2

Binder			Sand	Superplasticizer
Cement	Silica fume	Marble powder		
1	0.25	0.1	1.1	0.03

Table 3. Mix codes of RPC, steel-reinforced RPC (SFRPC), and PP-reinforced RPC (PFRPC) and the fiber contents

Mix code	Fibers	Content (% v/v)
RPC	Without fibers	0.00
SFRPC-1.00	Steel	1.00
SFRPC-1.50		1.50
SFRPC-2.00		2.00
PFRPC-0.10	PP	0.10
PFRPC-0.15		0.15
PFRPC-0.20		0.20

exceeding 2000 MPa. Meanwhile, the PP fibers were sourced from PT Indo Kordsa Tbk., West Java, Indonesia, featuring a length of 12 mm, a diameter of 0.27 mm, a tensile strength of 400 MPa, and a melting point of 160°C. Fig. 1 shows the physical appearance of both fiber types, emphasizing their entanglement differences.

2.2 Mix designs and curing

The RPC mix design is presented in Table 2. The dry constituents-cement, silica fume, and fine sand-were thoroughly blended in accordance with ASTM C305 (2020) to ensure homogeneous

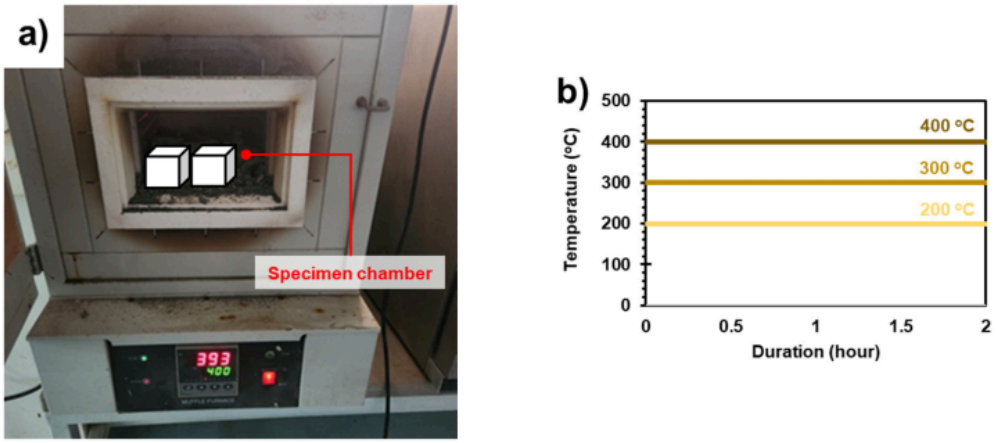

Figure 2. (a) Heating chamber used for thermal exposure and (b) temperature setting maintained for 2 hours

mixes. Subsequently, a water-superplasticizer solution was gradually introduced to achieve the desired workability, facilitating proper molding and compaction. After attaining uniformity, fibers were incorporated into designated mixes in varying proportions, as detailed in Table 3. The contents were chosen as the typical range of effective dosages for steel and PP fibers reported in the previous studies [22-24]. The fiber-containing mixes were further mixed until the fibers were evenly dispersed, ensuring optimal reinforcement integration. The prepared concrete was cast into 50×50×50 mm^3 cubes. The molded samples underwent a 28-day curing process in a moist environment before further testing. All experimental tests were performed in triplicate for each mix and exposure condition, and the reported results represent the average of three specimens.

2.3 Test methods

After the standard 28-day curing period to achieve maturity [5, 6, 25], the specimens were subjected to elevated temperature exposure in a controlled furnace at constant temperatures of 200°C, 300°C, and 400°C for 2 hours to simulate heat-induced thermal conditions. The selected temperature range was intended to investigate the progressive thermal response of RPC and to distinguish the temperature-dependent effects of steel- and PP-fiber reinforcement. The three exposure levels were used to systematically evaluate changes in spalling behavior and residual compressive strength from moderate to increasingly severe thermal exposure. Fig. 2 illustrates the setup for thermal exposure. The specimens were gradually cooled to room temperature overnight after the heating phase. After cooling, weight measurements and compressive strength tests were performed. The compressive strength tests were conducted in accordance with ASTM C109 (2023) to ensure accurate and standardized assessment of strength retention.

Using the obtained weight data, the spalling degree (SD) was determined using Eq. (1). In this equation, UW_{25} and UW_t represent the unit weight of the specimen at ambient temperature (25°C) and after exposure to a specific elevated temperature (t°C). The unit weight was calculated as the mass-to-volume ratio, with a constant specimen volume of 125 cm^3.

$$SD = \frac{UW_{25} - UW_t}{UW_{25}} \times 100\% \quad (1)$$

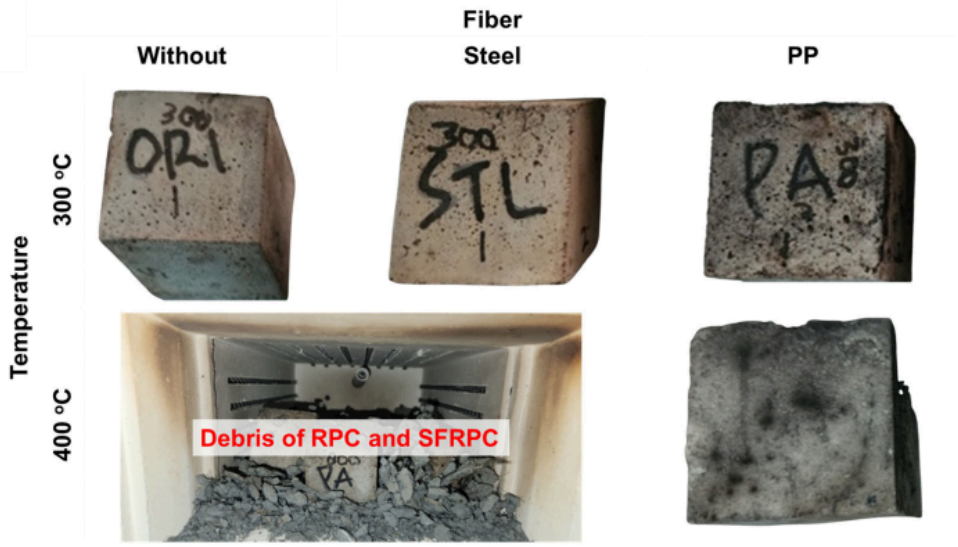

Figure 3. Representative condition of RPC, SFRPC, and PFRPC after exposure to elevated temperatures of 300°C and 400°C

3. Results and discussion

3.1 FRPC characterization

3.1.1 Spalling resistance

After exposure to elevated temperatures, no spalling was observed in the specimens heated to 200°C, indicating that the microstructural integrity of RPC and FRPC remained intact at this temperature. However, spalling became evident in samples subjected to 300°C and 400°C, as shown in Fig. 3. At 300°C, partial spalling was observed in both RPC and FRPC. When the temperature increased to 400°C, severe deterioration occurred. RPC and SFRPC underwent complete disintegration. In contrast, PFRPC exhibited superior thermal resistance, with only partial spalling occurring at 400°C. Soot-like carbon deposits were observed on the surface of PFRPC after exposure to this temperature. This observation demonstrates that PP fibers enhance RPC's resistance to spalling at higher temperatures up to 400°C.

Fig. 4 presents the quantified SD of FRPC reinforced with steel and PP fibers under varying temperature exposures. Small negative SD values were observed in some cases. According to Eq. (1), a negative SD value occurs when the measured unit weight after thermal exposure (UW_t) is slightly higher than the initial unit weight at 25°C (UW_{25}). Such small negative values may arise from experimental variation in the unit-weight measurements and are therefore interpreted as indicating negligible spalling. At 200°C, neither RPC nor FRPC exhibited spalling, indicating minimal thermal impact. However, at 300°C, SFRPC demonstrated improved spalling resistance compared to RPC, whereas PFRPC exhibited reduced resistance. At 400°C, the performance of SFRPC deteriorated drastically, leading to complete failure, similar to RPC. In contrast, PFRPC maintained superior spalling resistance despite its lower fiber content. The results highlight the effectiveness of PP fibers in enhancing RPC's thermal stability for high-temperature applications

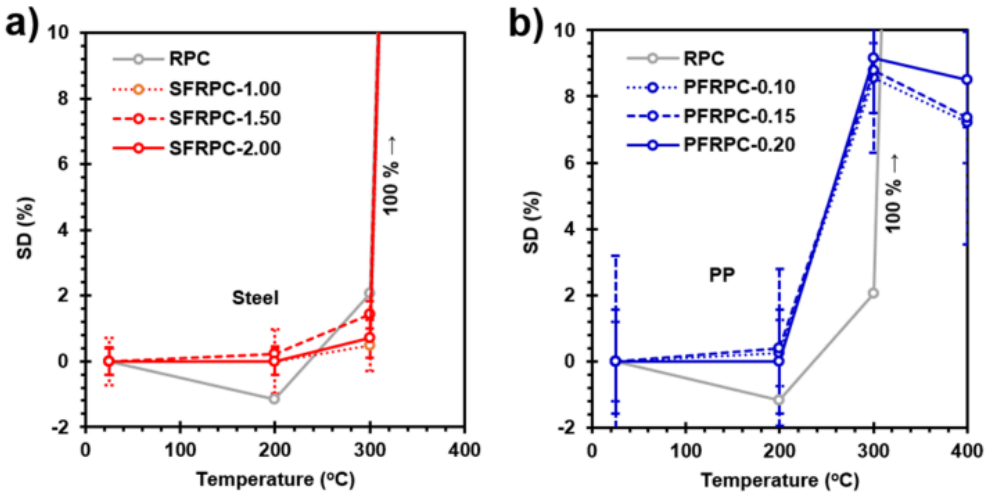

Figure 4. Spalling degree (SD) of specimens reinforced with (a) steel and (b) PP fibers

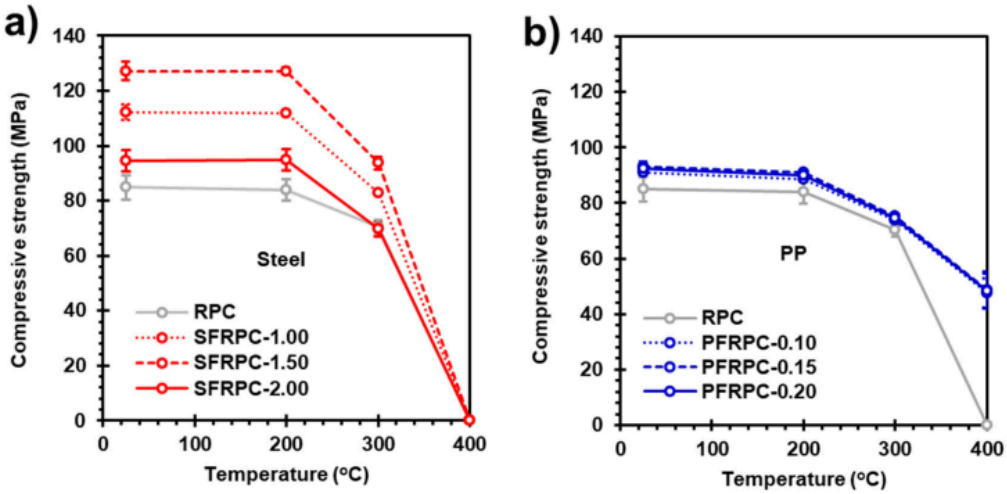

Figure 5. Compressive strength of (a) SFRPC and (b) PFRPC after exposure to elevated temperatures

above 300°C. The quantified SD values align with the observed physical deterioration, confirming the efficacy of steel fibers in mitigating spalling up to 300°C and the enhanced thermal resilience provided by PP fibers up to 400°C.

3.1.2 Compressive strength

Fig. 5 (a) and (b) illustrate the evolution of compressive strength in SFRPC and PFRPC under elevated temperature exposure. The inclusion of steel fibers improved the compressive strength of SFRPC, reinforcing its mechanical performance at ambient conditions and moderate temperatures up to 300°C. In contrast, PP fibers had a negligible effect on the initial compressive strength. Despite its early mechanical advantages, SFRPC experienced severe strength degradation at

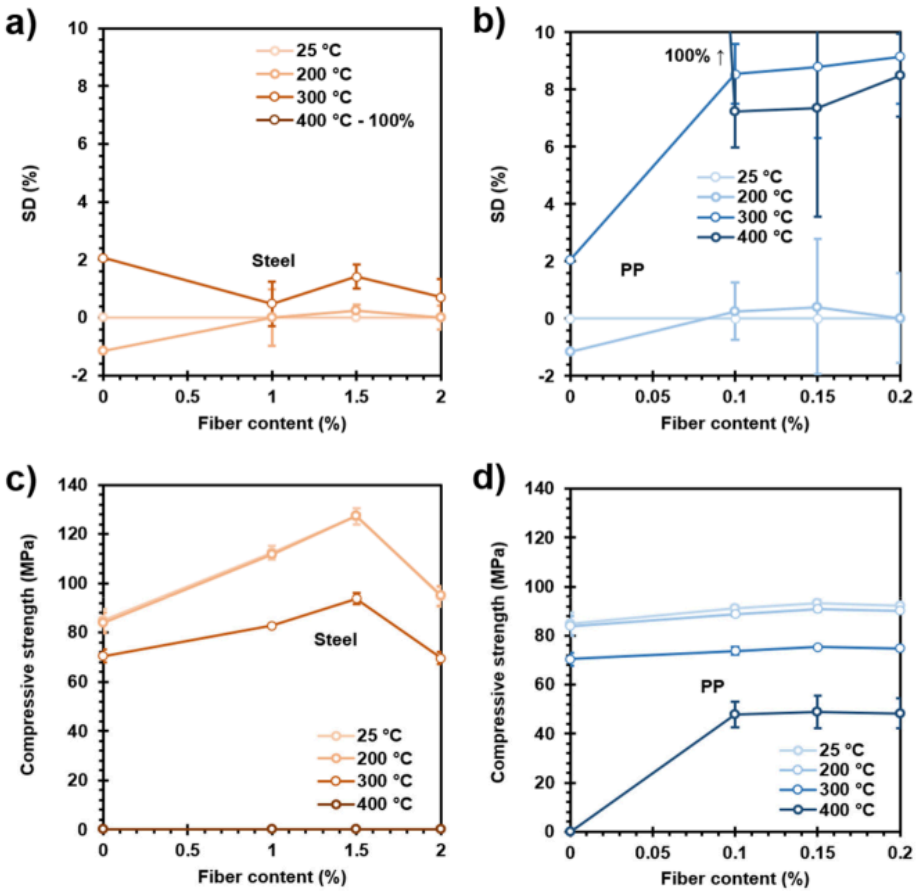

Figure 6. Influence of (a) steel and (b) PP fiber content on FRPC spalling. Impact of (c) steel and (d) PP fib content on FRPC compressive strength

400°C, ultimately leading to material failure. This sharp decline underscores the limitations of steel fibers in extreme thermal conditions. Conversely, PFRPC exhibited superior thermal resilience, effectively maintaining specimen integrity up to 400°C. The incorporation of PP fibers enhanced strength retention across the entire temperature range, highlighting their effectiveness in improving thermal resistance and stability beyond 300°C.

Overall, the findings indicate that while steel fibers initially enhance the mechanical properties of SFRPC, their effectiveness diminishes at higher temperatures, rendering PP fibers a more suitable choice for applications demanding superior thermal resistance and durability under extreme heat exposure beyond 300°C. These results provide valuable insights into the thermal performance and stability of FRPC, particularly in high-temperature environments. The selection of fiber type-steel or PP-plays a decisive role in governing the material's mechanical integrity and thermal resilience. Notably, the results from both spalling resistance and strength retention analyses consistently support the recommendation that steel fibers are suitable for applications up to 300°C, while PP fibers provide enhanced protection against heat-induced degradation beyond

this threshold.

3.1.3 Effective fiber content

In addition to selecting the appropriate fiber type, determining the optimal fiber content is crucial in designing FRPC for enhanced resistance to elevated temperatures. Fig. 6 shows the impact of fiber content on both spalling severity and compressive strength. The results exhibit a growth-and-decline pattern, indicating that the most effective fiber content depends on the performance criterion considered. In this study, the optimal fiber contents were identified as 1.00% for steel fibers and 0.10% for PP fibers for mitigating spalling, while the higher dosages (i.e., 1.50% for steel fibers and 0.15% for PP fibers) proved most effective in preserving compressive strength. However, the optimal content for spalling resistance became more pronounced at higher temperatures-300°C for steel fibers and 400°C for PP fibers-owing to the increasing significance of fiber functionality under extreme thermal exposure.

The optimization of fiber content relies on a delicate balance between its beneficial and detrimental effects [26]. The positive impact of fibers primarily stems from their crack-bridging ability and crack mitigation, which enhances the load-bearing capacity and toughness of FRPC [27]. This reinforcing effect is highly dependent on fiber properties, particularly their bonding efficiency within the cementitious matrix. However, surpassing the optimal fiber content can lead to diminished performance due to several adverse factors, including poor fiber dispersion, reduced workability, and increased porosity, all of which compromise the material's homogeneity and mechanical integrity [28, 29]. These findings underscore the critical need for precise optimization of fiber content for different fiber types to maximize thermal stability and mechanical performance. An appropriately selected fiber content can improve the overall performance of FRPC under elevated temperatures while mitigating the adverse effects associated with excessive fiber incorporation.

The variation in performance with fiber content further indicates that increasing fiber dosage does not necessarily result in proportional improvement, highlighting the importance of fiber distribution and fiber–matrix interaction. More broadly, the present findings demonstrate that the thermal performance of FRPC cannot be adequately evaluated using a single performance indicator. Exposure temperature, fiber type, fiber content, spalling resistance, and residual compressive strength collectively influence the overall response of FRPC. Therefore, these factors should be integrated into a comprehensive performance evaluation when selecting fiber type and content for elevated-temperature applications. The development of a unified performance parameter incorporating these factors may provide a useful approach for future optimization of FRPC, although appropriate normalization and weighting of the individual parameters would need to be established. These distinct temperature-dependent damage characteristics suggest different governing mechanisms for steel- and PP-fiber-reinforced RPC. Section 3.2 discusses the underlying physical and microstructural mechanisms responsible for these experimental observations.

3.2 Microstructural evolution

The spalling or disintegration observed in RPC and FRPC can be attributed to their microstructural evolution. Fig. 7 depicts the thermal response of the RPC matrix and fibers, linking microstructural transformations to crack propagation. The matrix is characterized by a densely compact, homogeneous structure with minimal porosity. The hydrated cement matrix

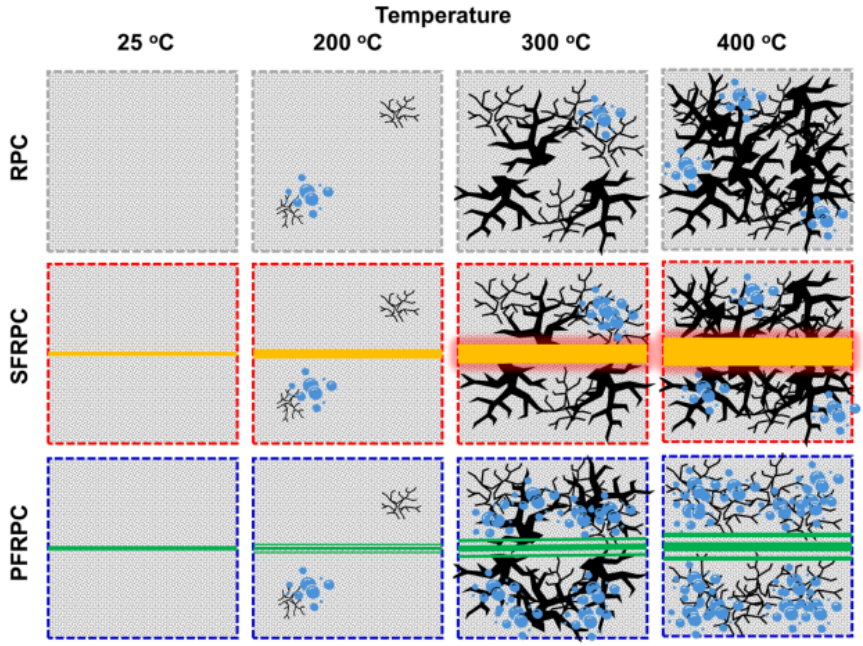

Figure 7. Temperature-dependent crack formation and vapor release in RPC, SFRPC, and PFRPC. Orange bars represent steel fibers, with red glow indicating oxide-layer formation; green bars represent PP fibers, with separated segments indicating melting; and blue bubbles represent released water vapor

contains free water within capillary pores (i.e., the interconnected, tiny voids or spaces within the matrix that are not filled by hydration products) and chemically bound water within hydration products [30]. At 25°C, hydration products, including calcium silicate hydrate (C-S-H), portlandite ($Ca(OH)_2$), ettringite, and monosulfate, are formed [31, 32]. Their stability and cohesive interactions play a crucial role in governing the matrix's mechanical strength and integrity.

As temperatures rise, water retained within the matrix and hydration products are gradually released over a broad thermal range (50-600°C), undergoing phase transitions as decomposition progresses [33]. Furthermore, the phase transition from liquid to vapor increases internal pore pressure [34, 35]. At 200°C, shrinkage begins as C-S-H loses chemically bound water, contributing to microcrack formation and reduced mechanical strength. By 300°C, C-S-H degradation continues, intensifying microcracking due to differential shrinkage between phases and further weakening the matrix. At 400°C, widespread C-S-H decomposition, coupled with the release of bound water from hydration products, accelerates pore expansion and propagates micro- to macro-cracking, resulting in severe strength loss.

As temperature increases, SFRPC undergoes microstructural evolution involving thermal expansion, oxidation, phase transformations, and progressive degradation of the fiber-matrix bond. At 200°C, steel fibers undergo thermal expansion, generating internal stresses within the matrix due to the mismatch in thermal expansion coefficients [36]. This differential expansion weakens the interfacial bond between the fibers and the matrix. Additionally, initial surface oxidation of steel fibers may commence, forming a thin iron oxide layer (e.g., Fe_2O_3 and Fe_3O_4) [37]. At 300°C, continued thermal expansion of the steel fibers exacerbates interfacial debonding from the

matrix, leading to more pronounced crack formation around the fibers due to increased internal stress. Oxidation accelerates, with iron oxides becoming more prominent on the fiber surface. By 400°C, the bond strength between steel fibers and the matrix deteriorates due to thermal mismatch and decomposition of hydration products [38]. The steel fibers experience surface roughening and form an oxide scale, with extensive oxidation. As the oxide layer thickens, the mechanical interlock between steel fibers and the matrix diminishes. Additionally, carbon may diffuse into the oxide layer, altering the steel's microstructural properties and further compromising its mechanical performance.

The microstructural evolution of PFRPC under elevated temperatures progresses through distinct stages, including softening, melting, decomposition, and pyrolysis of PP fibers. At 200°C, PP fibers begin to melt, forming voids [39]. This process generates capillary channels, enhancing permeability and reducing the risk of explosive spalling in high-temperature conditions. As temperature rises, PP fibers may further drain or redistribute within the matrix, with the polymer persisting in liquid form within microvoids. Heat-induced polymer chain scission accelerates degradation, releasing low-molecular-weight hydrocarbons and volatile organic compounds (VOCs) [40]. Oxygen-containing radicals further intensify decomposition. Ultimately, nearly all PP fibers degrade completely, leaving behind residual carbon deposits. The final byproducts depend on oxygen availability: in an oxygen-rich environment, oxidation produces carbon monoxide (CO) and carbon dioxide (CO_2), whereas in oxygen-deficient conditions, soot-like carbon is formed [41]. The enhanced thermal resistance of PFRPC at 400°C may be attributed to effective crack formation facilitated by PP fiber melting. The creation of numerous smaller cracks prevents the propagation of larger, more detrimental cracks, thereby preserving material integrity. Additionally, upon cooling, the residual molten PP may fill and bridge microcracks, further contributing to the thermal resilience.

These mechanisms explain the different spalling responses observed experimentally. Steel fibers primarily resist damage through crack bridging and restriction of crack propagation, which contributed to the improved spalling resistance of SFRPC at 300°C. Although thermal mismatch between the steel fibers and matrix may induce local microcracking, such cracks may not form sufficiently interconnected pathways to effectively relieve accumulated vapor pressure. With increasing temperature, deterioration of the matrix and fiber–matrix interface further reduces the crack-bridging effectiveness of steel fibers; consequently, at 400°C, this mechanical reinforcing mechanism was insufficient to prevent the severe deterioration observed in SFRPC. In contrast, melting of PP fibers creates additional voids and interconnected pathways that facilitate moisture and vapor transport, thereby reducing internal pressure. This pressure-relief mechanism provides a plausible explanation for the substantially better preservation of PFRPC specimen integrity at 400°C.

3.3 Consideration of steel and PP fibers

Table 4 presents a comparative analysis of steel and PP fibers in the design of FRPC incorporating marble powder, underscoring the critical role of fiber selection in enhancing thermal resistance. Steel fibers improved both spalling resistance and compressive strength, with an optimal fiber content of 1.00% for mitigating spalling and 1.50% for reserving strength. Steel fibers effectively enhanced load-bearing capacity and preserved mechanical performance in low to moderate temperature environments (up to 300°C). However, their effectiveness diminished at higher temperatures. Beyond 300°C, a pronounced decline in strength was observed, and at 400°C,

Table 4. Comparison of steel and PP fibers for design consideration of FRPC

Design consideration	Fibers	
	Steel	PP
Spalling resistance	• Optimal content: 1.00% • Resisting up to 300°C	• Optimal content: 0.10% • Resisting up to 400°C
Compressive strength	• Optimal content: 1.50% • Retaining up to 300°C	• Optimal content: 0.15% • Retaining up to 400°C

SFRPC experienced an abrupt and severe strength loss. These thermal constraints indicate that SFRPC is best suited for structural applications where sustained exposure does not exceed 300°C, ensuring reliable performance in moderate-temperature conditions.

Unlike steel fibers, PP fibers had a negligible impact on the compressive strength of FRPC under ambient conditions. However, they played a crucial role in enhancing the thermal resistance of FRPC, allowing it to withstand temperatures up to 400°C. With an optimal fiber content of 0.10% for spalling resistance and 0.15% for preserving strength, PP fibers contributed to material resilience under higher elevated temperatures beyond 300°C.

Considering the T-rating framework, which defines the maximum permissible surface temperature of equipment in hazardous environments, the experimental results provide a material-level indication of how the investigated FRPC systems behave at temperatures corresponding to selected T-class limits. The superior performance of SFRPC up to 300°C corresponds to the maximum surface-temperature limit associated with the T2 class. Under more severe thermal exposure beyond this limit, PP fibers provided greater resistance to spalling, with PFRPC maintaining its integrity at 400°C, a temperature approaching the 450°C maximum surface-temperature limit associated with the T1 class. This distinction is relevant where FRPC is considered as part of structural or protective construction surrounding equipment or hazardous areas: steel fibers provide greater mechanical reinforcement under moderate elevated-temperature exposure, whereas PP fibers provide greater protection against severe spalling as temperatures approach the T1 range.

From a practical perspective, these findings provide a basis for the comparative selection of fiber type and content in FRPC incorporating marble powder according to anticipated elevated-temperature exposure and required performance. However, the present recommendations are derived from material-level tests using 50×50×50 mm specimens under controlled constant-temperature exposure. The exposure temperatures of 300-400°C therefore represent the investigated elevated-temperature conditions and should not be interpreted as direct simulations of actual fire exposure or as established temperature limits for structural applications. Nevertheless, the results provide useful comparative evidence of the temperature-dependent behavior of the investigated fiber systems, particularly the transition from the greater effectiveness of steel fibers at 300°C to the better preservation of specimen integrity by PP fibers at 400°C.

Specimen size may influence the thermal response, as larger structural elements can develop greater temperature gradients between the exposed surface and interior, which may affect thermal stresses, moisture migration, vapor-pressure development, cracking, and spalling. Thermal history is also an important consideration because practical elevated-temperature exposure generally involves transient heating and cooling rather than constant-temperature exposure; consequently, variations in heating rate, exposure duration, peak temperature, and cooling conditions may alter the progression and severity of thermal damage. In real structural applications, these thermal

effects may be further influenced by structural dimensions, loading conditions, and restraint. Therefore, the findings of the present study should be considered as comparative material-level guidance for the selection of steel and PP fibers rather than direct validation of full-scale structural thermal performance. Further investigations using larger structural elements and representative thermal-exposure histories, including higher exposure temperatures, are required to extend and validate these findings for real-scale applications.

4. Conclusions

This study examined the spalling resistance and compressive strength of fiber-reinforced reactive powder concrete (FRPC) incorporating marble powder and reinforced with steel and polypropylene (PP) fibers at 200°C, 300°C, and 400°C. The findings reveal distinct fiber performance in mitigating thermal damage:

- At 200°C, neither steel nor PP fibers had a influence on spalling resistance.
- Up to 300°C, steel fibers provided superior spalling resistance, effectively maintaining the integrity of the RPC matrix.
- At 400°C, PP-reinforced RPC (PFRPC) exhibited enhanced thermal resistance, continuing to resist spalling and retain residual strength, whereas steel-reinforced RPC (SFRPC) experienced complete specimen disintegration.
- Optimal fiber contents were identified as 1.00% for steel and 0.10% for PP to maximize spalling resistance, while 1.50% for steel and 0.15% for PP were optimal for compressive strength retention. However, the influence of PP fibers on ambient compressive strength was negligible.

Based on these findings, steel fibers are recommended for applications where temperatures rise to 300°C, as they provide superior thermal resistance and mechanical stability. However, their rapid degradation beyond this threshold indicates the need for additional thermal protection measures under more severe elevated-temperature conditions. For applications exceeding 300°C, PP fibers are the preferred choice because they mitigate spalling and maintain structural integrity under extreme heat.

In relation to the T-rating framework, the effective performance of SFRPC up to 300°C corresponds to the maximum surface-temperature limit associated with the T2 class. At higher temperatures, PP fibers provided greater resistance to thermal deterioration and spalling, with PFRPC maintaining its integrity at 400°C, approaching the 450°C maximum surface-temperature limit associated with the T1 class. These findings provide useful material-level guidance for the selection of steel and PP fibers where FRPC is considered as part of structural or protective construction in thermally demanding or hazardous environments. Future research should extend these material-level findings to larger structural elements under representative transient thermal-exposure histories to evaluate the temperature-dependent effectiveness of steel and PP fibers at the structural scale and to support the development of practical guidance for the elevated-temperature performance of FRPC.

Acknowledgments

This research has been funded by the research grant awarded by Directorate of Research,

Technology, and Community Services of Directorate General of Higher Education, Research, and Technology under the Ministry of Education, Culture, Research, and Technology.

References

1. Ni, Z., Zhao, D., Tam, L.H., Lau, D., Chow, C.L. (2024). Fire safety performance of functional vegetated green building systems: a comprehensive review. Journal of Building Engineering, 98, 111200. https://doi.org/10.1016/j.jobe.2024.111200.
2. Karunaratne, T., Han, S., Lau, D., Chow, C.L. (2024). Experimental and numerical investigation of fire hazard of vertical greenery systems. Journal of Building Engineering, 95, 110004. https://doi.org/10.1016/j.jobe.2024.110004.
3. Bombardier, B. (2010). Ensure product safety with hazardous locations and solid-state lighting certification. 2010 IEEE symposium on product compliance engineering proceedings, 1-5.
4. Deng, J., Cui, J., Surahman, R., Tu, M., Wang, Y. (2025). Experimental and analytical study on heat transfer of concrete with different degrees of saturation under elevated temperatures. Fire and Materials, 49(3), 269-279. https://doi.org/10.1002/fam.3270.
5. Ahmed, S., Al-Dawood, Z., Abed, F., Mannan, M.A., Al-Samarai, M. (2021). Impact of using different materials, curing regimes, and mixing procedures on compressive strength of reactive powder concrete-A review. Journal of Building Engineering, 44, 103238. https://doi.org/10.1016/j.jobe.2021.103238.
6. Guo, M., Gao, R. (2021). Experimental comparability between steam and normal curing methods on tensile behavior of RPC. Advances in Concrete Construction, 11(4), 347-356. https://doi.org/10.12989/acc.2021.11.4.347.
7. Richard, P., Cheyrezy, M. (1995). Composition of reactive powder concretes. Cement and Concrete Research, 25(7), 1501-1511. https://doi.org/10.1016/0008-8846(95)00144-2.
8. Erdogdu, S., Kandil, U., Nayir, S. (2019). Effects of cement dosage and steel fiber ratio on the mechanical properties of reactive powder concrete. Advances in Concrete Construction, 8(2), 139-144. https://doi.org/10.12989/acc.2019.8.2.139.
9. Mayhoub, O.A., Nasr, E.S.A., Ali, Y.A., Kohail, M. (2021). The influence of ingredients on the properties of reactive powder concrete: a review. Ain Shams Engineering Journal, 12(1), 145-158. https://doi.org/10.1016/j.asej.2020.07.016.
10. Kushartomo, W., Wiyanto, H., Christianto. D. (2022). Effect of cement–water ratio on the mechanical properties of reactive powder concrete with marble powder as constituent materials. Proceedings of the 2nd international conference of construction, infrastructure, and materials: ICCIM 2021, Jakarta, Indonesia, July.
11. Demirel, B., Alyamaç, K.E. (2018). Waste marble powder/dust. Waste and Supplementary Cementitious Materials in Concrete, Woodhead Publishing.
12. Sai, A.N., Sakthivel, M., Arunvivek, G.K., Kumar, P., Dharmaraj, R., Sembeta, R.Y. (2026). Mechanical and durability assessment of marble dust–fiber concrete supported by ML prediction. Scientific Reports, 16(1), 10106. https://doi.org/10.1038/s41598-026-40874-z.
13. Kore, S.D., Vyas, A.K., Kabeer KI, S.A. (2020). A brief review on sustainable utilisation of marble waste in concrete. International Journal of Sustainable Engineering, 13(4), 264-279. https://doi.org/10.1080/19397038.2019.1703151.
14. Abbas, M.M., Muntean, R. (2025). Marble powder as a sustainable cement replacement: a review of mechanical properties. Sustainability, 17(2), 736. https://doi.org/10.3390/su17020736.
15. Ju, Y., Liu, J., Liu, H., Tian, K., Ge, Z. (2016). On the thermal spalling mechanism of reactive powder concrete exposed to high temperature: numerical and experimental studies. International Journal of Heat and Mass Transfer, 98, 493-507. https://doi.org/10.1016/j.ijheatmasstransfer.2016.03.033.
16. Shaikh, F.U.A., Taweel, M. (2015). Compressive strength and failure behaviour of fibre reinforced concrete at elevated temperatures. Advances in Concrete Construction, 3(4), 283-293. https://doi.org/

10.12989/acc.2015.3.4.283.
17. Ren, P., Hou, X., Kodur, V.K.R., Ge, C., Zhao, Y., Zhou, W. (2021). Modeling the fire response of reactive powder concrete beams with due consideration to explosive spalling. Construction and Building Materials, 301, 124094. https://doi.org/10.1016/j.conbuildmat.2021.124094.
18. Revathi, S., Brindha, D., Harshani, R. (2023). Effect of incorporating fibers in reactive powder concrete–a review. Materials Today: Proceedings. https://doi.org/10.1016/j.matpr.2023.04.472.
19. Ponikiewski, T., Katzer, J., Kilijanek, A., Kuźmińska, E. (2018). Mechanical behaviour of steel fibre reinforced SCC after being exposed to fire. Advances in Concrete Construction, 6(6), 631. https://doi.org/10.12989/acc.2018.6.6.631.
20. Mao, Z., Zhang, J., Luo, Z., Ma, Q., Duan, Y., Li, S., Miao, Y. (2021). Behavior evaluation of hybrid fibre-reinforced reactive powder concrete after elevated temperatures. Construction and Building Materials, 306, 124917. https://doi.org/10.1016/j.conbuildmat.2021.124917.
21. Raza, S. S., Qureshi, L. A., Ali, B., Raza, A., Khan, M. M. (2021). Effect of different fibers (steel fibers, glass fibers, and carbon fibers) on mechanical properties of reactive powder concrete. Structural Concrete, 22(1), 334-346. https://doi.org/10.1002/suco.201900439.
22. Zhong, C., Liu, M., Zhang, Y., Wang, J., Liang, D., Chang, L. (2020). Study on mechanical properties of hybrid polypropylene-steel fiber RPC and computational method of fiber content. Materials, 13(10), 2243. https://doi.org/10.3390/ma13102243.
23. Zhong, C., Liu, M., Zhang, Y., Wang, J. (2019). Study on mix proportion optimization of manufactured sand RPC and design method of steel fiber content under different curing methods. Materials, 12(11), 1845. https://doi.org/10.3390/ma12111845.
24. Zheng, W., Li, H., Wang, Y. (2012). Compressive behaviour of hybrid fiber-reinforced reactive powder concrete after high temperature. Materials & Design, 41, 403-409. https://doi.org/10.1016/j.matdes.2012.05.026.
25. Lee, M.G., Wang, Y.C., Chiu, C.T. (2007). A preliminary study of reactive powder concrete as a new repair material. Construction and Building Materials, 21(1), 182-189. https://doi.org/10.1016/j.conbuildmat.2005.06.024.
26. Dadmand, B., Pourbaba, M., Sadaghian, H., Mirmiran, A. (2020). Effectiveness of steel fibers in ultra-high-performance fiber-reinforced concrete construction. Advances in Concrete Construction, 10(3), 195-209. https://doi.org/10.12989/acc.2020.10.3.195.
27. Lin, C., Kanstad, T., Jacobsen, S., Ji, G. (2023). Bonding property between fiber and cementitious matrix: a critical review. Construction and Building Materials, 378, 131169. https://doi.org/10.1016/j.conbuildmat.2023.131169.
28. Sharma, R., Jang, J.G., Bansal, P.P. (2022). A comprehensive review on effects of mineral admixtures and fibers on engineering properties of ultra-high-performance concrete. Journal of Building Engineering, 45, 103314. https://doi.org/10.1016/j.jobe.2021.103314.
29. Nuaklong, P., Chittanurak, J., Jongvivatsakul, P., Pansuk, W., Lenwari, A., Likitlersuang, S. (2020). Effect of hybrid polypropylene-steel fibres on strength characteristics of UHPFRC. Advances in Concrete Construction, 10(1), 1-11. https://doi.org/10.12989/acc.2020.10.1.001.
30. Jennings, H.M., Bullard, J.W., Thomas, J.J., Andrade, J.E., Chen, J.J., Scherer, G.W. (2008). Characterization and modeling of pores and surfaces in cement paste: correlations to processing and properties. Journal of Advanced Concrete Technology, 6(1), 5-29. https://doi.org/10.3151/jact.6.5.
31. Scrivener, K., Ouzia, A., Juilland, P., Mohamed, A.K. (2019). Advances in understanding cement hydration mechanisms. Cement and Concrete Research, 124, 105823. https://doi.org/10.1016/j.cemconres.2019.105823.
32. Bullard, J.W., Jennings, H.M., Livingston, R.A., Nonat, A., Scherer, G.W., Schweitzer, J.S., ... Thomas, J.J. (2011). Mechanisms of cement hydration. Cement and Concrete Research, 41(12), 1208-1223. https://doi.org/10.1016/j.cemconres.2010.09.011.
33. Scrivener, K., Snellings, R., Lothenbach, B. (2018). A practical guide to microstructural analysis of cementitious materials. CRC Press.
34. Ye, L.I., Zhang, D., Tan, K.H. (2020). On measuring techniques of pore pressure in concrete at elevated

temperature. Cement and Concrete Composites, 114, 103737. https://doi.org/10.1016/j.cemconcomp.2020.103737.

35. Drouet, E., Poyet, S., Torrenti, J.M. (2015). Temperature influence on water transport in hardened cement pastes. Cement and Concrete Research, 76, 37-50. https://doi.org/10.1016/j.cemconres.2015.05.002.
36. Khaliq, W., Kodur, V. (2011). Thermal and mechanical properties of fiber reinforced high performance self-consolidating concrete at elevated temperatures. Cement and Concrete Research, 41(11), 1112-1122. https://doi.org/10.1016/j.cemconres.2011.06.012.
37. Shadi, A.M.H., Kamaruddin, M.A., Niza, N.M., Emmanuel, M.I., Hossain, M.S., Ismail, N. (2020). Efficient treatment of raw leachate using magnetic ore iron oxide nanoparticles Fe_2O_3 as nanoadsorbents. Journal of Water Process Engineering, 38, 101637. https://doi.org/10.1016/j.jwpe.2020.101637.
38. Zhang, Y., Ju, J.W., Chen, Q., Yan, Z., Zhu, H., Jiang, Z. (2020). Characterizing and analyzing the residual interfacial behavior of steel fibers embedded into cement-based matrices after exposure to high temperatures. Composites Part B: Engineering, 191, 107933. https://doi.org/10.1016/j.compositesb.2020.107933.
39. Zeiml, M., Leithner, D., Lackner, R., Mang, H.A. (2006). How do polypropylene fibers improve the spalling behavior of in-situ concrete? Cement and Concrete Research, 36(5), 929-942. https://doi.org/10.1016/j.cemconres.2005.12.018.
40. Li, Z., Wei, X., Liu, J., Han, H., Jia, H., Song, J. (2021). Mechanical properties and VOC emission of hemp fibre reinforced polypropylene composites: natural freezing-mechanical treatment and interface modification. Fibers and Polymers, 22(4), 1050-1062. https://doi.org/10.1007/s12221-021-0052-8.
41. Jakes, K.A., Drews, M.J. (1981). On the role of oxygen in the horizontal flame spread of polypropylene. Journal of Polymer Science: Polymer Chemistry Edition, 19(8), 1921-1936. https://doi.org/10.1002/pol.1981.170190805.

Thermal resistance of fiber-reinforced reactive powder concrete with marble powder waste

ORIGINALITY REPORT

18%	19%	10%	0%
SIMILARITY INDEX	INTERNET SOURCES	PUBLICATIONS	STUDENT PAPERS

PRIMARY SOURCES

1	www.techno-press.com Internet Source	11%
2	files.bilpubgroup.com Internet Source	7%
3	mdpi-res.com Internet Source	1%
4	renewal.techno-press.org Internet Source	1%

Exclude quotes	On	Exclude matches	< 1%
Exclude bibliography	On		

Thermal resistance of fiber-reinforced reactive powder concrete with marble powder waste

GRADEMARK REPORT

FINAL GRADE

/100

GENERAL COMMENTS

PAGE 1

PAGE 2

PAGE 3

PAGE 4

PAGE 5

PAGE 6

PAGE 7

PAGE 8

PAGE 9

PAGE 10

PAGE 11

PAGE 12

PAGE 13

PAGE 14

PAGE 15

PAGE 16